



Article

# First Report of Leaf Spot Disease (“Negrilla”) on *Agave salmiana* Otto Ex Salm-Dyck (ssp. *salmiana*) Plants Caused by *Bipolaris zeae* Zivan in Mexico

Teresa Romero-Cortes <sup>1</sup>, Victor H. Pérez España <sup>1</sup>, José A. Pescador-Rojas <sup>1</sup>, Eduardo Rangel-Cortés <sup>2</sup>, María M. Armendariz-Ontiveros <sup>1</sup> and Jaime A. Cuervo-Parra <sup>1,\*</sup>

<sup>1</sup> Escuela Superior de Apan, Universidad Autónoma del Estado de Hidalgo, Carretera Apan-Calpulalpan, Km 8, Chimalpa Tlalayote, Apan 43900, Mexico; romero@uaeh.edu.mx (T.R.-C.); victorhugo\_perez@uaeh.edu.mx (V.H.P.E.); josealfredo\_pescador@uaeh.edu.mx (J.A.P.-R.); maria\_armendariz@uaeh.edu.mx (M.M.A.-O.)

<sup>2</sup> Facultad de Ciencias, Universidad Nacional Autónoma de México, Investigación Científica, C. U. Coyoacán, Ciudad de México 04510, Mexico; erangel@ciencias.unam.mx

\* Correspondence: aliascha@uaeh.edu.mx; Tel.: +52-771-717-2000 (ext. 5805 or 5806)

**Abstract:** *Agave* genera include slow-growing plants with cultural and economic roots dating back to pre-Columbian times in Mexico. Several species have a widespread presence in the country and are cultivated and/or used directly from the field to obtain various derived products. *Agave salmiana* is widely used in the region of the High Valleys of Apan, Hidalgo, Mexico. However, fungal diseases are causing considerable losses to *Agave* crops. For this reason, fungi strains from maguey plants from Apan, Hidalgo, with “Negrilla” disease symptoms were isolated and identified morphologically and molecularly. The results provide information on a new disease disseminated in *A. salmiana* plants, which causes symptoms such as black spots on the leaves due to pathogenic fungi of the genera *Bipolaris*. The morphological and molecular characterization located the phytopathogenic fungus as new isolates of *Bipolaris zeae*. Finally, the re-isolation of the causal agent of the disease was achieved in all pathogenicity tests, verifying that the symptoms observed in the maguey plants were caused by *B. zeae*, thus corroborating Koch’s postulates, and constituting the first report of this fungus as a pathogen of *A. salmiana* in Mexico.

**Keywords:** *Agave salmiana*; *Bipolaris*; *Cochliobolus*; Helmintosporidae; leaf spot



**Citation:** Romero-Cortes, T.; Pérez España, V.H.; Pescador-Rojas, J.A.; Rangel-Cortés, E.; Armendariz- Ontiveros, M.M.; Cuervo-Parra, J.A. First Report of Leaf Spot Disease (“Negrilla”) on *Agave salmiana* Otto Ex Salm-Dyck (ssp. *salmiana*) Plants Caused by *Bipolaris zeae* Zivan in Mexico. *Agronomy* **2024**, *14*, 623. <https://doi.org/10.3390/agronomy14030623>

Academic Editor: Francesco Calzarano

Received: 20 February 2024

Revised: 8 March 2024

Accepted: 18 March 2024

Published: 20 March 2024



**Copyright:** © 2024 by the authors. Licensee MDPI, Basel, Switzerland. This article is an open access article distributed under the terms and conditions of the Creative Commons Attribution (CC BY) license (<https://creativecommons.org/licenses/by/4.0/>).

## 1. Introduction

The *Helminthosporium* complex [1] includes the phytopathogen graminicolous fungi species and the most important genera are *Drechslera*, *Bipolaris*, and *Exserohilum* [2]. The *Bipolaris* Shoemaker genera [3] and their *Cochliobolus* Drechsler [4] sexual morph [5] are opportunistic and pathogenic microorganisms with a worldwide distribution, which are present in air, soil, and plants [6]. The *Bipolaris* species generally have pale, multiseptate, straight or curved conidia, without the presence of bulges in their cells. The *Cochliobolus* presents structures with an oscillate ascoma, pseudo paraphyses and bitunicate asci; and within its ascus, one typically finds the multiseptate and filiform ascospores with helical shape arrangement [1,7]. These pathogenic fungi are commonly associated with several disease symptoms, such as leaf spots and blights, melting out, and root and foot rot, reproducing mainly in crop plants of high economic value [1,8–12]. Crops such as wheat (*Triticum* spp.), corn (*Zea mays*), and rice (*Oryza sativa*) exhibit serious losses in grain yields due to diseases caused by some *Bipolaris* species [13–15]. Additionally, the *Bipolaris* and *Cochliobolus* species occur ubiquitously and are saprophytic and pathogenic to more than 60 plant host genera [16]. Similarly, these fungi cause human diseases such as dermatomycosis, keratitis, allergic sinusitis, central nervous system infections, disseminated infections, etc. [17–20]. However, the pathologies in humans caused by representatives of these genera

are very infrequent, occurring only in patients with serious problems in their immune system [21].

The *Bipolaris* classification based on morphological characters was initially complicated because some species shared characteristics of morphology (sexual and asexual) with the genera *Curvularia* [8]. In addition, the conidia and the conidiophores are highly variable within species [22]. In an attempt to solve the conflict in the nomenclature for these two genera, much research has focused on molecular phylogenetics to relocate many species on the genera *Bipolaris* in *Curvularia* [5,6,23,24], which is helpful for establishing the correct location of new fungal isolates within the *Bipolaris* and *Curvularia* group [25,26]. In Mexico, different *Bipolaris* species have been registered as foliar pathogens of crops such as oat (*Avena sativa* L.), wheat, rice, barley (*Hordeum vulgare*), and maize [10,13,27–29]. Given that the genera *Bipolaris* has more than 60 species, each one with different physiological, phytopathological, biochemical, and biological characteristics [1,30], it is important its proper identification to control and manage diseases produced by these fungi complex group, as well as to identify disease symptomatology in plants that have not been previously infected. In this sense, Perez-España et al. [12] reported that the *Agave salmiana* plants present a fungal disease that is characterized by the existence of circular gray spots on the leaves, which become necrotic over time. These results are in agreement with Hernández et al. [31] study, where they reported the same symptomatology for the same *Agave* species caused by the etiological agent of *Curvularia lunata*, this study was carried out in different municipalities of Hidalgo, Mexico. Therefore, the identification of species involved in causing the symptomatology observed in *Agave* plants is an attractive alternative for mitigating, controlling, and preventing diseases produced by pathogenic fungi. As managing diseases in *Agave* plants is desirable, this research aims to morphologically and molecularly identify the causal agent of the “leaf spot” disease in *A. salmiana* plants and determine the pathogen(s) aggressiveness isolated in plants of the genera *Agave* cultured under field conditions.

## 2. Materials and Methods

### 2.1. Fungal Strains Isolation

Fungi strains were isolated from the cuticle layer of *Agave salmiana* with disease symptoms in the form of dark black spots (colloquially called “Negrilla” in Mexico) during the years 2019, 2020, and 2021 from the municipality of Apan, Hidalgo, Mexico, (19°39'20" LN and 98°31'05" LW, 2488 masl), under rainfed conditions. Samples were sterilized by immersion in a 3% sodium hypochlorite solution for 60 s, followed by two washes in sterile distilled water; dried on filter paper; and then placed on Petri dishes containing potato dextrose agar (PDA, Bioxon®, Becton Dickinson, Edomex, Mexico) in a moist chamber. A total of eight fungal strains were isolated and selected based on the characteristics developed during their culture. Fungi were incubated under dark conditions at 28 °C for one week [32] or until the colony covered the entire culture medium [10]. Subsequently, the selected growing colonies were subcultured on PDA under the same conditions until its analysis.

### 2.2. Morphological Characterization

Macroscopic morphological identification of the eight strains was performed on PDA and Sabouraud Dextrose Agar (SDA, DifcoTM, Sarks, MD, USA) culture media. Subsequently, the strains were morphologically identified at the macroscopic level, and the PDA medium was used to create the descriptions of microscopic structures. The strain identification was based on the comparisons with other *Bipolaris* strains [1,5,11,33] and complemented with new observations. Fifty measurements for each trait observed in each isolated species were made to calculate the length and width of the following structures: ascocarps, conidiophores, conidia, and the number of dictyoseptae per conidia. The morphological measurements were made with a compound microscope (Leica DM 3000, Leica Microsystems GmbH, Wetzlar, Germany) using bright field and a scanning electron microscope (SEM) (JEOL, Model IT300, Boston,

MA, USA) both located at the Escuela Superior de Apan (ESAp-UAEH), Hidalgo, Mexico. The photographs were digitally generated using the CorelDraw 2017 software (CorelDRAW Graphics Suite, version 2017, Mexico City, Mexico).

### 2.3. Molecular Characterization

The genomic DNA from each strain was extracted using the Sanger sequencing method (Eurofins Genomics GmbH, Ebersberg, Germany). The strains DNA extraction was carried out following the methodology described by Cuervo-Parra et al. [34]. The PCR reactions and amplifications were performed in an automatic thermal cycler (Techne PRIME3, Series No. 31309, Cole Parmer, Staffordshire, UK), as described by Romero-Cortes et al. [35]. The amplicons were recovered and washed twice with TE buffer (Tris HCl 10 mM, EDTA 1 mM). The gene internal transcribed spacers, which contained the ITS I/5.8s/ITS II region of the ribosomal DNA (rDNA), were amplified using the primers ITS1 and ITS4 [36]. The purified PCR products were sequenced by Cinvestav-IPN (Irapuato, Mexico). The DNA sequences were assembled using the ChromasPro 2.1.10.1 software (Technelysium Pty Ltd, South Brisbane, Australia) and aligned with the BLAST® 2.15.0 software from the NCBI GenBank database [37]. The sequences were deposited in the GenBank database with the accession numbers ON630338 to ON630345. The phylogenetic analyses were performed by generating a tree with the Neighbor-joining statistic method (NJ), using the Tajima-Nei model, supported with the bootstrap test of the phylogeny method, using 1000 random replicates with the MEGA X 10.2.2 software [38].

### 2.4. Pathogenicity Tests

To comply with Koch's postulates [39], healthy one-year-old *Agave* seedlings from healthy adult maguey plants were planted in an experimental plot, under a completely randomized experimental design, and experimental evaluation began one month after plant establishment [40]. Each experimental treatment consisted of six *A. salmiana* seedlings with 7 to 8 leaves sowed and inoculated with *Bipolaris zeae* (strain JCP-N07) in leaves and rhizosphere under field conditions. The pathogenicity experimental field was prepared with a substrate composed of sand (80 kg), limestone (120 kg), and black soil (200 kg) from the previous crop cycle. The experiment was performed in triplicate using 21 *Agave* seedlings as non-inoculated controls (T1) and 21 *Agave* seedlings inoculated with *Bipolaris zeae* (T2) in the year 2022.

The *Agave* plant inoculation with *B. zeae* was based on the technique modification described by Mata-Santoyo et al. [13]. To infect the *A. salmiana* plants of the spot leaf disease, a solution containing 15 mL in equal volumes of a  $5 \times 10^6$  conidia/mL and Tween 80 (1%) of *B. zeae* strain JCP-N07 in sterile distilled water was sprayed directly onto the leaves and rhizosphere of each *Agave* plant of T2. The T1 plants were sprayed with sterile distilled water. The evaluation began five days after the inoculation, according to the severity scale proposed by Perelló et al. [41], where 1 = free of infection; 2 = 1 to 5%; 3 = 5 to 12%; 4 = 12 to 20%; 5 = 20 to 35%; 6 = 35 to 45%; 7 = 45 to 60%; 8 = 60 to 80% and 9 = more than 80% of the leaf area was affected with necrosis and generalized chlorosis. The data obtained were converted to percentages and an ANOVA analysis of variance was performed using the Statistix 10.0 software [42] and the means were compared by Tukey's HSD All-Pairwise test at a significant difference ( $p < 0.05$ ).

## 3. Results and Discussion

### 3.1. Morphological Characterization

The fungal colonies isolated and selected from *A. salmiana* plants, cultivated in PDA medium, showed a diameter of 44.8 to 45 mm ( $44.9 \pm 0.1$  mm) in 7 days at 28 °C, with an average of 6.41 mm per day. On the other hand, the colonies in the SDA medium reached a diameter between 44.9 and 45 mm ( $44.96 \pm 0.05$  mm) in 6 days at 28 °C, with an average of 7.49 mm per day. The fungal colonies color was initially white in the two different culture media (PDA and SDA), turning to olive green over time, and then changing to dark black in

PDA medium (Figure 1A,B). In SDA medium, the colonies color changed from light brown to dark brown with the presence of some depressions (Figure 1C,D). The velvety texture in both media PDA and SDA was due to the presence of conidia. After 7 days of growth, the presence of pustules was observed, and the colonies showed a cottony texture, changing from olive green to dark gray (Figure 1A,B) and light gray (Figure 1C) over time in PDA and SDA culture media, respectively. The colonial growth observed was rosette-shaped (Figure 1A) to radial (Figure 1B) in PDA, and radial (Figure 1C,D) in SDA. The back colonies were black in PDA and SDA (Figure 1E,F). However, in SDA, the presence of striae is due to the folds observed on the front of the colonies (Figure 1F).

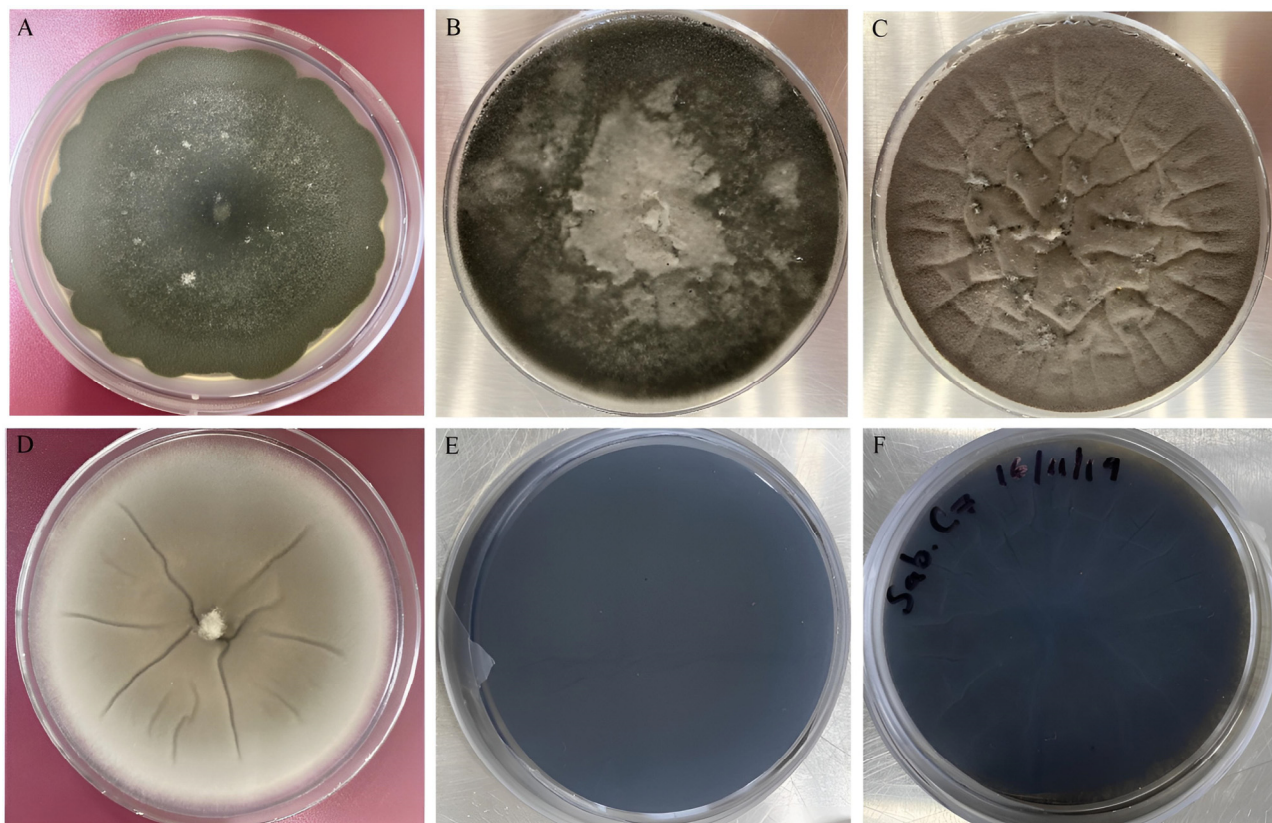


**Figure 1.** *Bipolaris zeae* morphology in PDA and Sabouraud medium. (A,B) Pustules showing morphological and color variations in PDA after 7 days, as well as growth ranging from rosette to radial. (C,D) Few pustules grew on the mycelium with a cracked appearance due to the great abundance of folds observed in SDA medium. Reverse colony morphology (E) in PDA and (F) in SDA culture media.

The fungi of the *Cochliobolus* genera are characterized by presenting brown conidiophores and conidia, straight or curved fusoid, and their germination occurs from a germ tube at each end [6]. In this sense, the colonies in the Petri dishes had abundant sporulation after 7 days. The hyphae observed were septate, branched, and smooth, with a thickness up to 7  $\mu\text{m}$ , and could be warty sometimes [1]. The conidiophores were abundant, cylindrical, straight, or flexuous, geniculated at the upper part, smooth, dark brown, arising singly or sometimes in small groups, branched, septate (Figure 2A,B), with size of 80.67–372  $\mu\text{m}$  long  $\times$  6.02–8.1  $\mu\text{m}$  wide (av. = 222.15  $\mu\text{m}$ , SE = 110.02,  $n$  = 50, long; av. = 7.5  $\mu\text{m}$ , SE = 0.64,  $n$  = 50, wide). The conidiogenous nodes were dark below, with a smooth to slightly roughened surface. The conidia observed was 43–225  $\mu\text{m}$  long  $\times$  12.02–22  $\mu\text{m}$  wide (av. = 124.34  $\mu\text{m}$ , SE = 57.31,  $n$  = 50; av. = 16.19  $\mu\text{m}$ , SE = 2.24,  $n$  = 50), straight to slightly curved, smooth, obclavate to fusiform, hyaline to olivaceous brown when immature and brown to reddish brown when mature (Figure 2C–E), with end cells usually paler than middle cells, sometimes presenting

Y-shaped conidia in PDA medium [6], with 6 to 14 distoseptate (av. = 9.3, SE = 2.52,  $n$  = 50), with the terminal cells cut by a thick dark septum, straight to slightly curved. The hilum was truncated, slightly protruding, 3–5  $\mu\text{m}$ . In the *Bipolaris* fungi, the conidia septum ontogeny was observed as follows: the first-formed septum is median to submedian, the second septum delimits the basal cell of the mature conidium, and the third septum delimits the distal cell [1].

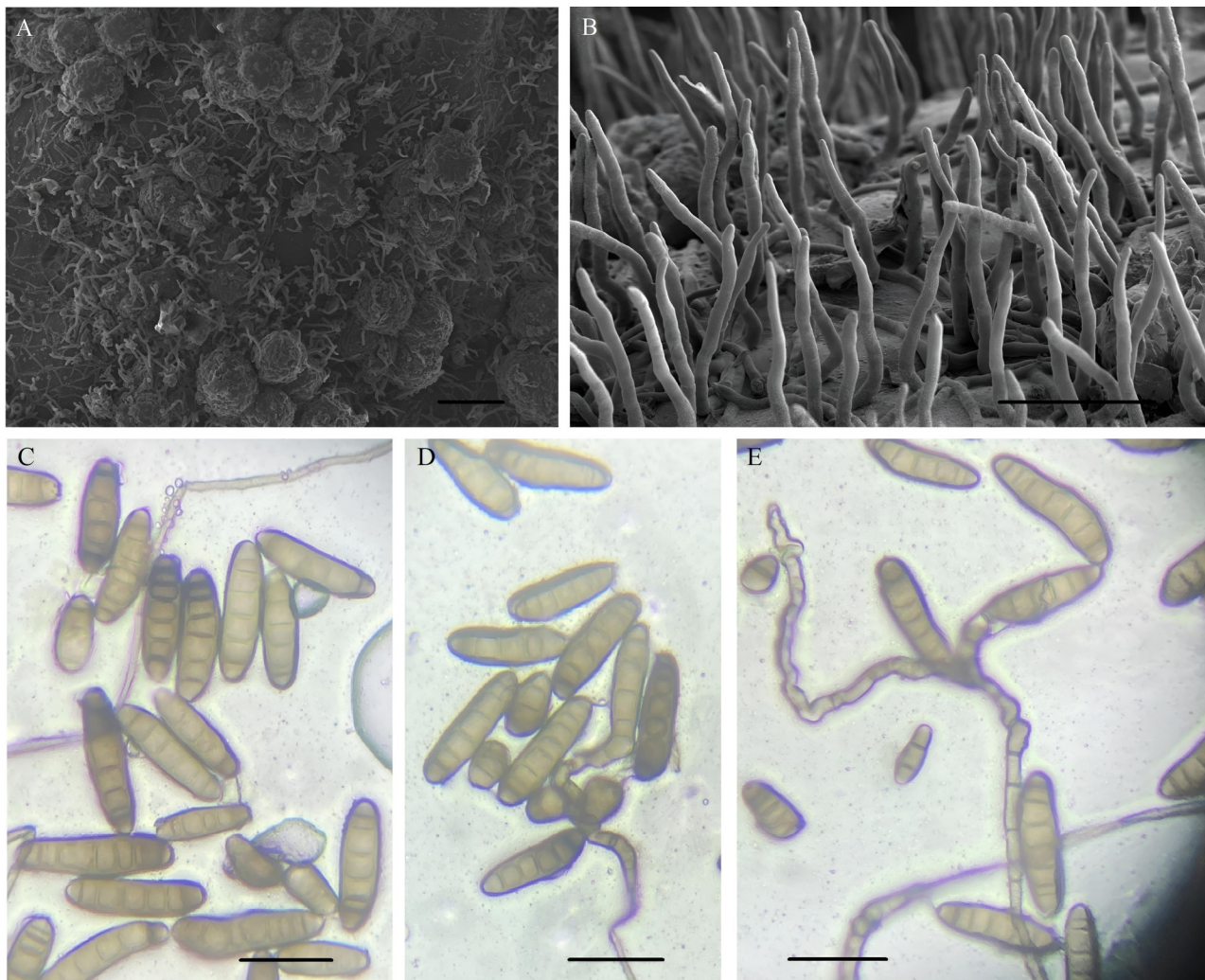


**Figure 2.** *Bipolaris zae* morphology in plant and PDA medium. (A,B) SEM ascomata and several conidiophores growing on the maguey leaf. (C–E) Conidia with 3-7-distoseptate, and conidiophore shape in PDA. Scale bars: (A) = 100  $\mu\text{m}$ , (B) = 50  $\mu\text{m}$ , (C–E) = 20  $\mu\text{m}$ .

Additionally, on the *A. salmiana* leaves with the previously described disease symptoms of leaf spots, an additional unusual type of conidia was observed (Figure 3A,B), which was lecythiform, verrucose, septate, with a size of 31.02–24.56  $\mu\text{m}$  long  $\times$  13.72–17.85  $\mu\text{m}$  wide (av. = 27.31  $\mu\text{m}$ , SE = 2,  $n$  = 50, long; av. = 16.20  $\mu\text{m}$ , SE = 1.32,  $n$  = 50, wide) arising from single conidiophores (Figure 3C–E) or in small groups (Figure 3F), with a morphology similar to that observed in PDA culture medium. The differences observed were in their size, between 72.38–79.75  $\mu\text{m}$  long  $\times$  3.58–5.57  $\mu\text{m}$  wide (av. = 76.78  $\mu\text{m}$ , SE = 2.38,  $n$  = 50, long; av. = 4.85  $\mu\text{m}$ , SE = 0.74,  $n$  = 50, wide) and the bilateral branching at its base from the main hypha, with one or more than three conidiophores in the same hypha, distributed over the ascomata (Figure 3A) and to the surface of the cuticular layer with disease symptoms (Figure 3B).

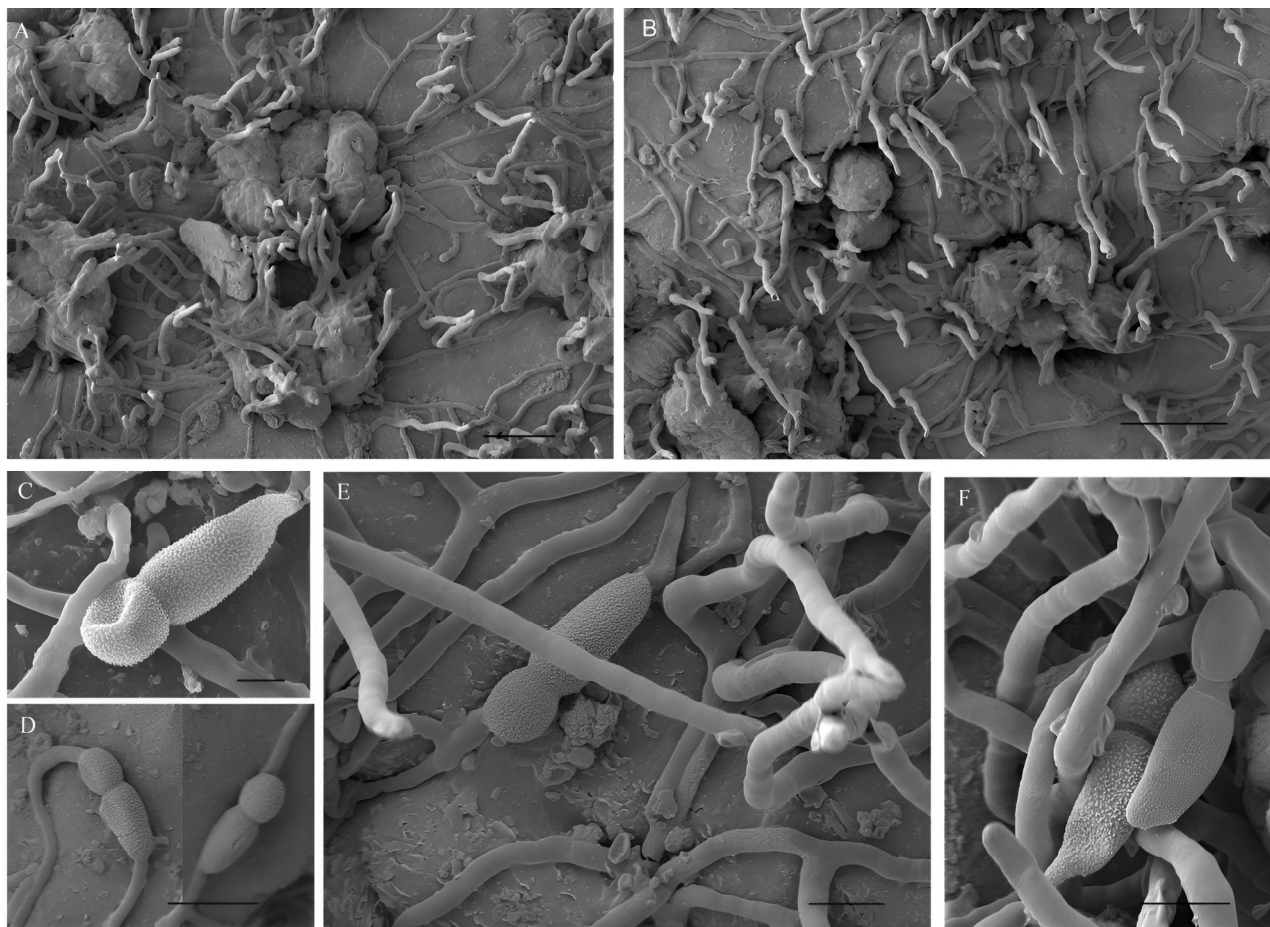


**Figure 3.** *Bipolaris zeae* colonies on maguey plants. (A,B) SEM ascomata with abundant conidiophores emerging from them, as well as hyphae with conidiophores on the maguey leaf. (C–F) SEM conidia and conidiophore morphological structures produced on the maguey leaf. Scale bars: (A,B) = 50  $\mu\text{m}$ , (C) = 5  $\mu\text{m}$ , (D) = 20  $\mu\text{m}$ , (E,F) = 10  $\mu\text{m}$ .

The following sexual morphological characteristics were observed in PDA: the ascomata were globose, black with a well-defined ostiolar neck, the size was 318–510  $\mu\text{m}$  long  $\times$  335.3–440  $\mu\text{m}$  wide (av. = 427.86  $\mu\text{m}$ , SE = 50.94,  $n$  = 50, long; av. = 398.73  $\mu\text{m}$ , SE = 38.66,  $n$  = 50, wide; Figure 3A,B). The ascii were thin-walled, cylindrical to broadly clavate, sessile or with a pedicel, with 4–8 ascospores packed helically in an ascus, 150–210  $\mu\text{m}$  long  $\times$  18–20  $\mu\text{m}$  wide, with filiform, hyaline, 6–8 septate ascospores, 260  $\mu\text{m}$  long  $\times$  6–8  $\mu\text{m}$  wide [6]. Similarly, the pseudoparaphyses were hyaline, filiform, and septate. The morphological characteristics of the conidiophores observed in the maguey plants were like those previously observed and described in PDA medium. The morphological characteristics of the different structures observed and the measurements obtained in this research permitted the identification of the studied strains as new *B. zeae* records from Mexico [6,11,33]. In addition, these results constitute the first report of this species as a pathogen of *A. salmiana* plants in the municipality of Apan, Hidalgo, in Mexico.

On the other hand, Figure 4A shows the formation of the *Cochliobolus zeae* ascomata. It was possible to observe the different stages of development of this structure in PDA medium. At the beginning of the colonial development (24 to 48 h), groups of hyphae with septa were observed growing on the culture medium (Figure 4B). Seven days after development, the hyphae began to intertwine with each other, giving rise to the formation of prosenchyma (Figure 4C). Subsequently, when the hyphae lost their individuality, they gave rise to the formation of a pseudoparenchyma (Figure 4D). Finally, the process of formation of the ascomata started when the pseudoparenchyma closed on itself (Figure 4E).

Regarding the *A. salmiana* leaves, when the conidia germinate, the hypha penetrates the interior of the cuticle via the stomata ostioles (Figure 4F). After some time, the ascomata begins to emerge from the cuticle layer through the stomata (Figure 4G), an action that directly interferes with the exchange of gases and water. When the ascomata has reached its maximum size, it begins to produce conidiophores and hyphae. The hyphae first develop on the cuticle adjacent to the affected stomata (Figure 4H) and begin the conidiophores production, leading to conidia formation (Figure 4I).

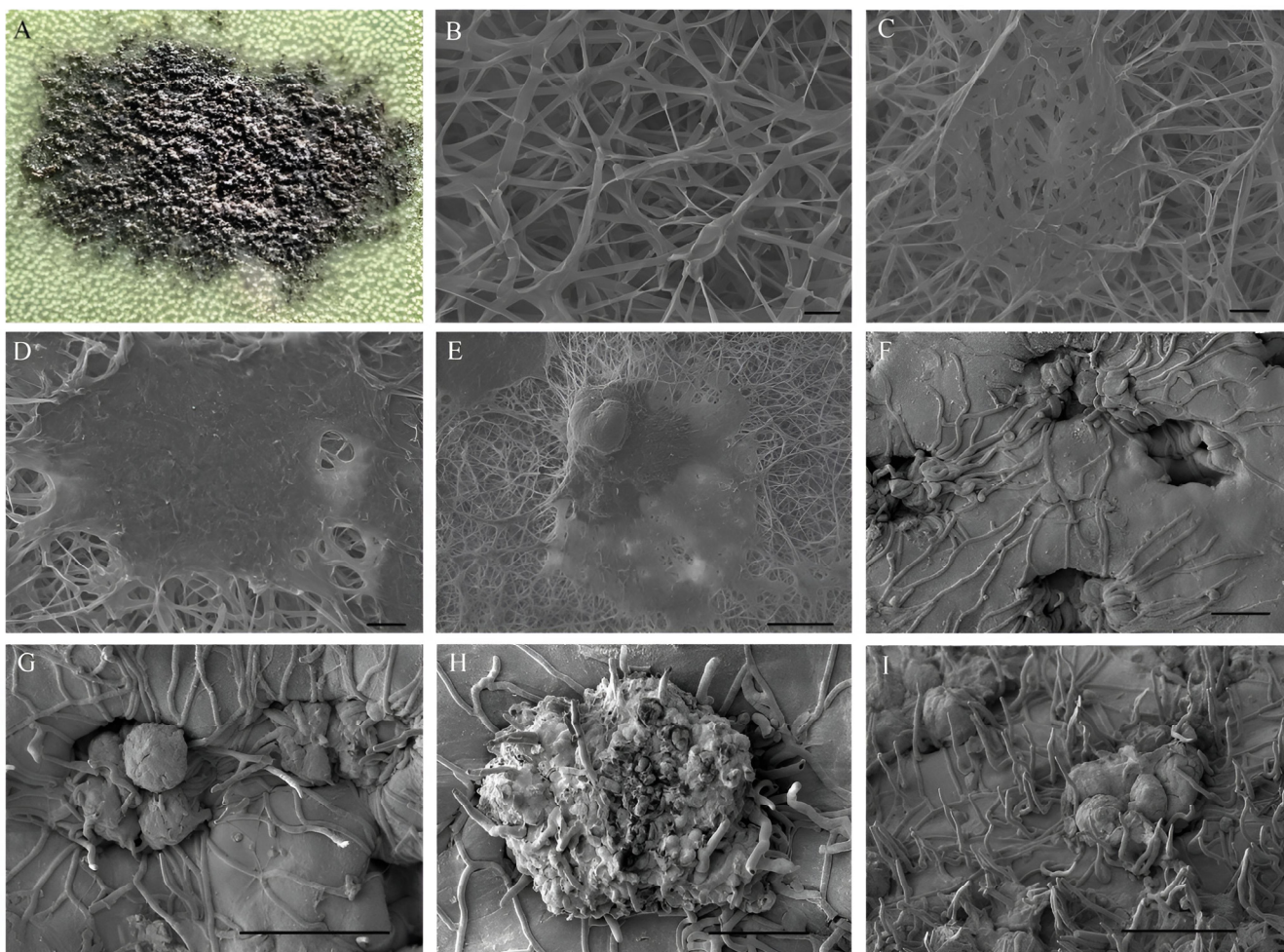


**Figure 4.** *Cochliobolus zeae* ascomata morphology in *Agave salmiana* (A,F–I) and in PDA medium (B–E). Macroscopic morphology of the leaf spot disease observed in maguey leaves (A). Set of hyphae with the presence of septa (B). Intertwined hyphae begin to form prosenchyma (C). Hyphae that have lost their individuality give rise to pseudoparenchyma (D). Pseudoparenchyma in the ascomata process forming (E). Hyphae enter the interior of the cuticle via stomata ostioles (F). Ascomata emerging from the stoma (G). Fully formed ascomata with hyphae growing on the left (H). Groups of ascomata with abundant hyphae and conidiophores growing on the maguey leaf (I). Scale bars: (B) = 10  $\mu$ m; (C,D) = 20  $\mu$ m; (F,H) = 50  $\mu$ m; (E,G,I) = 100  $\mu$ m.

It was possible to observe ascomata with abundant conidiophores production on the abaxial side of the cuticle layer of the longitudinal section of *A. salmiana* leaves with *C. zeae* leaf spot disease symptoms, which come out through the stomata, presenting abundant hyphae (Figure 5A). Also, abundant mycelium grew through the stomata on the adaxial side of the cuticle layer in different sections of the same affected maguey leaf (Figure 5B). In addition, when the cuticle layer was mechanically removed, it was possible to observe the mycelium growth in the inner tissue cells of the *A. salmiana* leaves (Figure 5C).

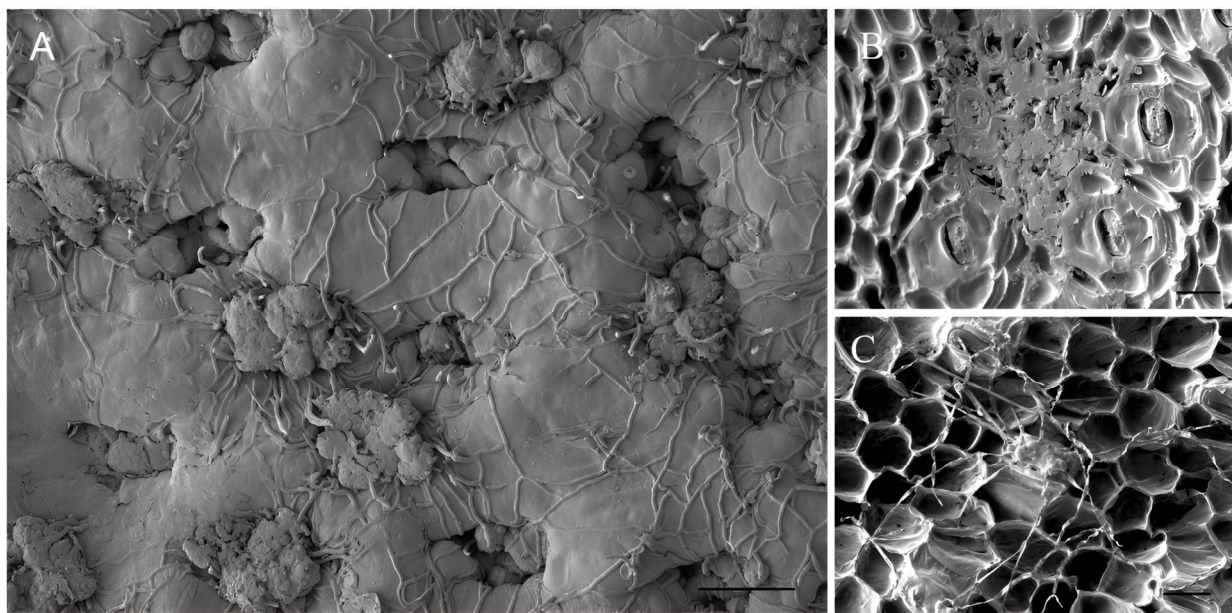


**Figure 5.** *Cochliobolus* colonies grown on *Agave salmiana* plant observed in SEM. (A) Ascomata with abundant hyphae and conidiophores emerge from the stomas on the adaxial side of the maguey leaf. (B) Mycelium growing through the stomas by the adaxial side of the cuticular layer from the maguey leaf. (C) Mycelium growing inside the internal parts of the stroma of the maguey leaf without the cuticular layer. Scale bars: (A) = 100  $\mu\text{m}$ , (B) = 50  $\mu\text{m}$ , (C) = 50  $\mu\text{m}$ .

In other plant species, such as *Pennisetum clandestinum*, *Setaria italica*, *Agropyron scabri-folium*, *Sorghum* spp., *Cenchrus ciliaris*, *Z. mays*, *Brachiaria brizantha*, *Setaria sphacelata*, *Triticum* spp., *Triticum aestivum*, and *A. sativa* [43], *B. zeae* causes necrotic spots on leaves like those observed on the leaves of *A. salmiana* in this study. Also, additional damage caused by *B. zeae*, such as root system lesions, has been reported in *Panicum maximum* plants under greenhouse trials [44]. For its part, *B. zeae* causes brown spots in *Fagopyrum esculentum*, most commonly on the lower leaves, where the spots initially were light brown with an irregular border and pale brown center, and older spots become dark brown and often coalesced [11]. Small, irregular, pale-brown lesions on middle and lower leaves were found on *Hemarthria altissima*, which became dark brown to yellow over time, spreading to all parts of the plant [45]. Other *Bipolaris* species, such as *Bipolaris microstegii*, also cause ellipsoidal to irregular leaf spots in *Microstegium vimineum* plants, which are brown with a darker near-black border [46]. On the other hand, leaf spots caused by several *Bipolaris* species in maize are distinct from those observed in other plant hosts, with elongated strip lesions, or fusiform, elliptical lesions caused by *Bipolaris maydis*, or narrow linear lesions caused by *Bipolaris zeicola*, and subrotund lesions caused by *Bipolaris saccharicola* [47].

On the other hand, other fungi have been reported as possible pathological agents in several species of the *Agave* genera. For example, *Epicoccum sorghinum* has been reported as a possible pathogen in *Agave tequilana* Weber var. blue plants [48,49], *A. angustifolia* [50], and *A. lechuguilla* [51]. Also, the fungus *Myrmaecium rubricosum* has been isolated from *A. tequilana* plants [52] and *A. lechuguilla* [53]. Another genus of fungi responsible for causing rot in maguey plants buds is the fungus *Fusarium lactis* isolated from *A. salmiana* plants [54,55]. Finally, the fungus *Curvularia lunata* has been isolated from plants of *Agave fourcroydes* [56] and *A. salmiana* [31,57] plants, causing typical leaf spots of the disease known as “Negrilla” in other municipalities of the state of Hidalgo in Mexico.

### 3.2. Molecular Characterization

The nucleotide sequences of the rDNA and the internal transcribed spacer are useful tools for the identification and classification of the different species of fungi that may be present in a crop [58]. In this research, a total of eight new nucleotide sequences

of phytopathogenic fungi belonging to the genera *Bipolaris* were characterized, together with additional sequences downloaded from the NCBI GenBank. For the amplification of the ITS I/5.8s/ITS II region of the rDNA of the phytopathogenic fungi isolated and identified morphologically in this study, the ITS1 (TCCGTAGGTGAACCTGCGG) and ITS4 (TCCTCCGCTTATTGATATGC) primers were used [36,59]. The length of the amplified sequences of the fungal strains isolated from *A. salmiana* plants ranged between 525 and 553 bp and were deposited in the NCBI GenBank database. The sequences pairwise analysis generated an identity percentage between 99.44 and 99.6%; this analysis was performed with the BLAST program [60] for the fungal sequences isolated from *A. salmiana* plants and other related *Bipolaris* sequences from GenBank. The BLAST analysis confirmed the previous morphological identification of the eight strains isolates from *A. salmiana* leaf tissue with black spots, thus placing all the isolates within the *Bipolaris* genera, corresponding to new isolates of *B. zeae* for Mexico (Table 1).

**Table 1.** Fungal identity based on sequencing of the ITS I/5.8s/ITS II region of rDNA.

Strain	Strain Accession	Species	Total Score	Query Cover (%)	Identity (%)	Accession Closest Hit	Accession Length (pb)	References
JCP-N01	ON630338	<i>B. zeae</i>	1003	100	99.64	MT505870	863	Visagie et al. [61]
JCP-N02	ON630339	<i>B. zeae</i>	985	100	99.63	MT505870	863	Visagie et al. [61]
JCP-N03	ON630340	<i>B. zeae</i>	976	100	99.63	MT505870	863	Visagie et al. [61]
JCP-N04	ON630341	<i>B. zeae</i>	976	100	99.44	MT505870	863	Visagie et al. [61]
JCP-N05	ON630342	<i>B. zeae</i>	959	100	99.62	MT505870	863	Visagie et al. [61]
JCP-N06	ON630343	<i>B. zeae</i>	985	100	99.63	MT505870	863	Visagie et al. [61]
JCP-N07	ON630344	<i>B. zeae</i>	1011	100	99.64	MT505870	863	Visagie et al. [61]
JCP-N08	ON630345	<i>B. zeae</i>	968	100	99.62	KJ909787	568	Manamgoda et al. [6]

The sequences selected for this study had a length between 467 and 863 pb and the length of the consensus sequence for the multiple sequence alignment was 876 bp. The phylogenetic analysis was performed for the ITS I/5.8s/ITS II region of the rDNA, including the partial sequences of the 18S and 28S ribosomal genes, for both *Bipolaris* and *Cochliobolus* selected strains. The analysis with the NJ statistical method of the Mexican *B. zeae* sequences and 27 other related sequences from GenBank generated a tree (Figure 6). The phylogenetic analysis revealed three main clades (I, II, and III) and three individual sequences located at the phylogenetic tree base, represented by sequences from the genera *Bipolaris* and *Cochliobolus*, supported by the bootstrap method phylogeny test, using 1000 random replicates. The tree was rooted with the *Curvularia spicifera* GenBank sequence MH864011 as an outgroup to infer phylogenetic relationships [62]. The best tree, which has a total branch length = 0.15517150, is shown.

At the top of clade I of the phylogenetic tree, the Mexican *B. zeae* sequences isolated from the *A. salmiana* plants were located in two branches with bootstrap values of 99 and 97, obtained by the NJ method during the phylogenetic analysis, together with the phylogenetically related sequences of *B. zeae* from the NCBI GenBank database that were isolated from different species of cultivated plants of the families Asteraceae, Polygonaceae, and Poacea from South Africa [61], Canada [63], China [11], and the United States of America [6,64].

In the middle part of clade I, the two sequences of *Bipolaris mediocris* and the individual sequence of *Bipolaris variabilis* were located. The first two were isolated from the Netherlands [62] and the third one was isolated from the leaf spots on *Pennisetum clandestinum* in Argentina [33]. All these sequences were supported by a bootstrap statistic value of 99. At the bottom of clade I, three *Bipolaris sorokiniana* sequences were located, supported by a bootstrap value of 90. The first one was isolated from grass plants of the genera *Lolium* in the Solomon Island [5] and the other two sequences were isolated from barley seeds

(*Hordeum vulgare*) with leaf spot symptoms [10]. It is worth mentioning that these two *B. sorokiniana* sequences and the other 14 sequences of fungi belonging to the leaf spot complex of barley were previously isolated in the same location in which the eight *B. zeae* strains were isolated in this study.



**Figure 6.** Phylogenetic analysis generated for *Bipolaris* from a Neighbor-joining analysis based on the ITS alignment. The numbers in the nodes are the bootstrap values.

Finally, along with the *B. sorokiniana* sequences, one *B. zeicola* sequence isolated from *Arachis hypogaea* (groundnut) plants from South Africa, was in an individual branch [65]. Within clade II, the sequences of *Cochliobolus microlaenae* and *Bipolaris peregranensis* were in the same branch, with a bootstrap value of 73. The first one was isolated from China and the second one from Australia, and both were found in *Cynodon dactylon* plants [16]. In a sister branch with a bootstrap value of 67, the *Cochliobolus chloridis* and the *Bipolaris cynodontis* sequences were located, both isolated in Australia; the first one was from *Chloris gayana* plants [16] and the second one was from *C. dactylon* plants [5]. In another nearby branch, five *Bipolaris oryzae* sequences were located, all of them isolated in Thailand from *Oryza sativa* plants [5], with a bootstrap support value of 91. These three branches in turn had a bootstrap statistical support of 56 (Figure 6).

On the other hand, the sequences of *Cochliobolus victoriae* (anamorph: *Bipolaris victoriae*) were in clade III, isolated from *A. sativa* plants and the sequence of *Cochliobolus carbonum* (anamorph: *B. zeicola*); the first one was isolated in the USA [16] and the second one was isolated in Canada [8], supported by a bootstrap value of 73. Finally, at the bottom of the phylogenetic tree, the sequences of *Cochliobolus melinidis*, *Cochliobolus sativus* (anamorph: *B. sorokiniana*), and *Cochliobolus heterostrophus* (anamorph: *B. maydis*) were located as individual isolates, the first one isolated from China [16] and the other two from Canada [66,67]. It is important to comment that all these sequences correspond to different species of fungi of the genera *Bipolaris/Cochliobolus* that cause pathologies in one or several plant species with economic importance to humans [1]. The isolated *Agave* strains selected the *A. salmiana* plants as a new host, and they presented similar symptoms to those observed in other plant species attacked by different strains of *B. zeae* [6,11,45,68]. This result is probably attributed to the nucleotide changes observed in the sequences of *B. zeae* isolated from *A. salmiana* plants with respect to the other sequences of *B. zeae* isolated from different plant species obtained from the NCBI GenBank database. Finally, the sequence of *C. spicifera* was located at the phylogenetic tree base as an external group [62].

### 3.3. *Bipolaris zeae* Pathogenicity Tests

Once the *B. zeae* strain was isolated and characterized, an aqueous solution containing a high concentration of this strain ( $5 \times 10^6$  conidia/mL) was prepared and sprayed onto *Agave* plants. Ninety days after the application of conidia suspension, all inoculated plants (T2) presented disease symptoms, showing foliar intensity damage of  $10.92 \pm 0.12a$ , considered as severe levels. The T1 plants did not present any disease symptoms in this period. The low severity levels observed in T2 plants may be explained by the chemical and structural composition of the maguey leaves, in relation to the quantity of epidermal cells, cutin, polysaccharides, waxes, and stomata present [12,69,70]. Figure 7D shows that all tissues of maguey leaves are invaded after a certain time, even though it takes a longer time for the *B. zeae* hyphae to colonize and invade the cuticle layer of maguey plants.

To confirm that the leaf spot symptoms observed in the *A. salmiana* seedlings were caused by the *B. zeae* conidia, samples of the infected tissues were taken and incubated in PDA medium, obtaining *B. zeae* colonies with the same morphological characteristics described above (Figure 8A). On the other hand, 20 days after *B. zeae* conidia inoculation, hyphae in different stages of development were observed emerging from the stomata on the maguey leaves of T2 plants (Figure 8B). Finally, it was possible to observe a completely developed ascocarps with the presence of several formed conidiophores, around 40 to 50 days after inoculation (Figure 8C).

The species *B. zeae* were morphologically identified and molecularly characterized to corroborate, at a molecular level, the correct identity of the fungus isolated from the infected maguey plants in the pathogenicity test. The results of the pairwise alignment of sequences, with the Blast program, gave a percentage of identity of 100% with the accession ON630344 corresponding to the JCP-N07 strain of *B. zeae* (Table 1), which was used in this research to carry out the pathogenicity experiments. Additionally, this sequence was published in the GenBank database with OR553122 as the accession number. This pathogenicity test and the molecular characterization confirm that *B. zeae* is the etiological agent of leaf disease symptoms observed in the evaluated maguey plants. In this regard, other species of the *Bipolaris* genera such as *B. maydis* and *B. zeicola* cause similar symptoms in corn crops [71] and *Curvularia verruculosa* and *C. lunata* in *A. lechuguilla* plants [72,73].

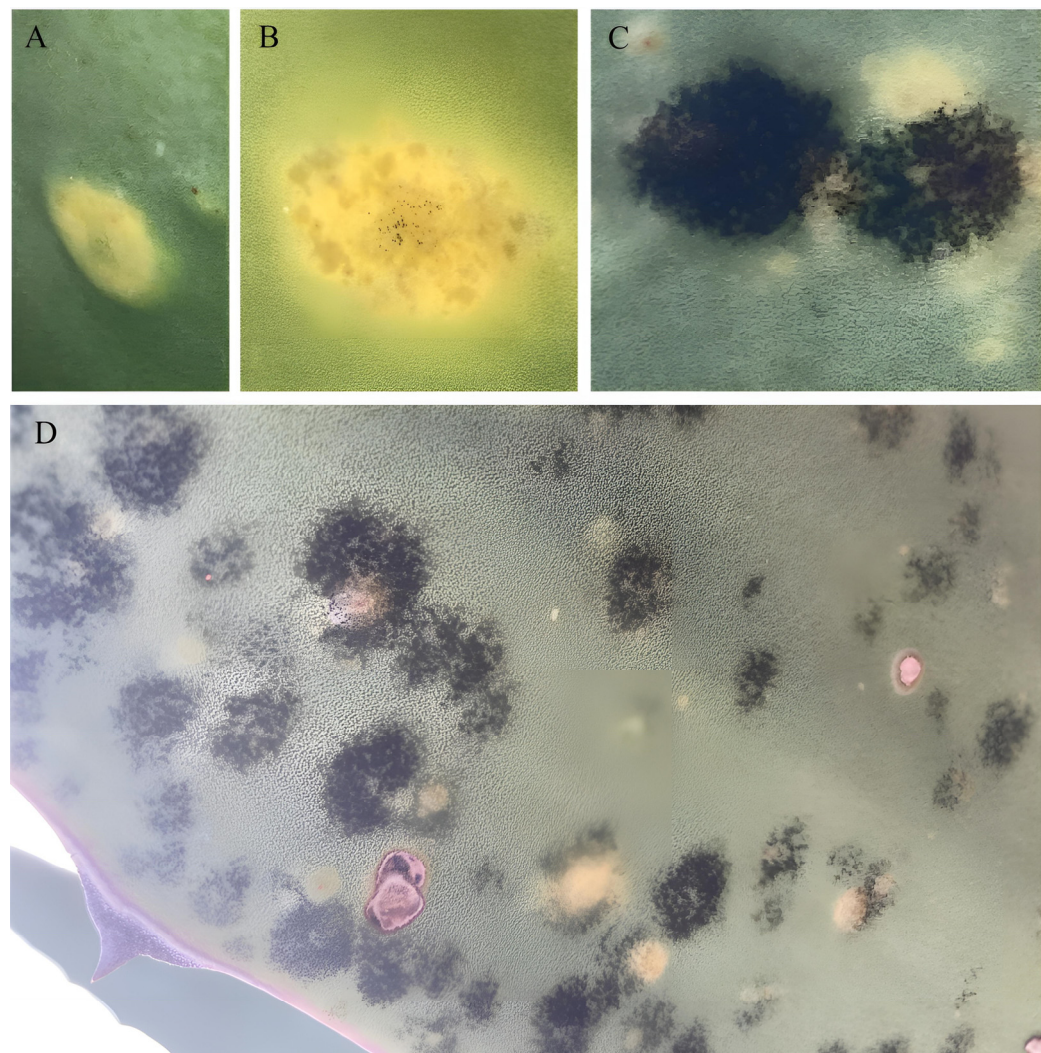


**Figure 7.** Leaf spots observed on the leaves of maguey plants. Early leaf spot symptoms on maguey leaves (**A**). Leaf spot observable symptoms in maguey leaves from 30 to 35 days of inoculation (**B**). Leaf spot developed on the *Agave* leave two months after starting the inoculation (**C**). Adult maguey leaf with *B. zeae* colonies, 5 months after the onset of the first symptoms (**D**).

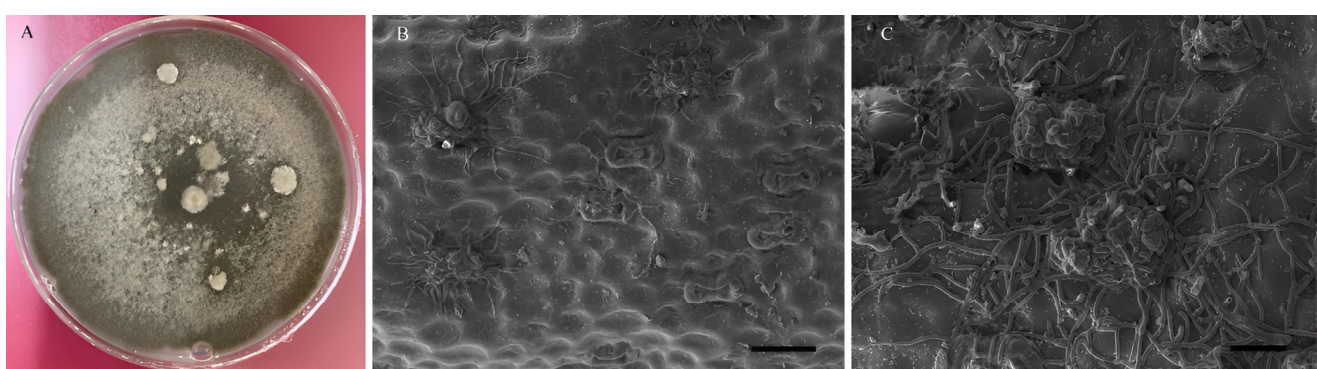


**Figure 8.** Leaf spot caused by *Bipolaris zeae* in plant and PDA medium. (**A**) *B. zeae* morphological characteristics observed in PDA after 7 days of growth. (**B,C**) Micrographs of ascospores in different development stages and conidiophores growing on the maguey leaf cuticle. Scale bars: (**B**) = 100  $\mu$ m, (**C**) = 50  $\mu$ m.

#### 4. Conclusions

*Agave salmiana* has high economic and cultural importance in Mexico. Pathogens are an area of interest for *Agave* producers and researchers due to the losses they cause in *Agave* plantations and production. *Agave* pathogens tend to spread to other crops, since maguey plantations are usually among forage plants, grain, and cereal crops, and for this reason, pathogens are studied extensively. The genera *Bipolaris* have a cosmopolitan distribution, frequently found in the leaves, stems, and roots of different grasses. The results presented in this paper confirm that the fungus *Bipolaris zeae* participates in leaf spot disease (colloquially called “Negrilla”) observed on the leaves of *Agave salmiana* plants. It is expected that these findings could provide more insight for creating practice strategies (cultural practice, chemical control, or biological agents) to control pathogens propagation among crops in the region. Also, further study into other pathogens related to this disease, such as *Curvularia lunata* and *C. verruculosa*, is recommended.

**Author Contributions:** Conceptualization, J.A.C.-P. and T.R.-C.; methodology, J.A.C.-P.; software, J.A.C.-P.; validation, J.A.C.-P., V.H.P.E., J.A.P.-R., E.R.-C., M.M.A.-O. and T.R.-C.; formal analysis, J.A.C.-P.; investigation, J.A.C.-P., V.H.P.E. and T.R.-C.; resources, J.A.C.-P., V.H.P.E., J.A.P.-R., E.R.-C. and T.R.-C.; data curation, J.A.C.-P. and T.R.-C.; writing—original draft preparation, J.A.C.-P.; writing—review and editing, J.A.C.-P., V.H.P.E., J.A.P.-R., E.R.-C., M.M.A.-O. and T.R.-C.; visualization and supervision, J.A.C.-P. and T.R.-C.; project administration, J.A.C.-P. and T.R.-C. All authors have read and agreed to the published version of the manuscript.

**Funding:** This research received no external funding.

**Data Availability Statement:** Data are contained within the article.

**Acknowledgments:** All the authors thank the staff of the Escuela Superior de Apan-UAEH for having provided all the facilities required to carry out the field and laboratory experiments. We also appreciate the support of JJ. Pelayo-Cárdenas for his help checking and improving the English language of the final manuscript.

**Conflicts of Interest:** The authors declare no conflicts of interest and the funders had no role in the design of the study; in the collection, analysis, or interpretation of data; in the writing of the manuscript; or in the decision to publish the results.

#### References

1. Sivanesan, A. *Graminicola Species of Bipolaris, Curvularia, Drechslera, Exserohilum and Their Teleomorphs*, 10th ed.; No. 158; CAB International Mycological Institute: Wallingford, UK, 1987; pp. 10–267.
2. Cardona, R.; González, M.S. Caracterización y patogenicidad de hongos del complejo *Helminthosporium* asociados al cultivo del arroz en Venezuela. *Bioagro* **2008**, *20*, 141–145.
3. Shoemaker, R.A. Nomenclature of *Drechslera* and *Bipolaris*, grass parasites segregated from ‘*Helminthosporium*’. *Canad. J. Bot.* **1959**, *37*, 879–887. [[CrossRef](#)]
4. Drechsler, C. Phytopathological and taxonomical aspects of *Ophiobolus*, *Pyrenophora*, *Helminthosporium* and a new genus *Cochliobolus*. *Phytopathological* **1934**, *24*, 973.
5. Manamgoda, D.S.; Cai, L.; McKenzie, E.H.C.; Crous, P.W.; Madrid, H.; Chukeatirote, E.; Shivas, R.G.; Tan, Y.P.; Hyde, K.D. A phylogenetic and taxonomic re-evaluation of the *Bipolaris*–*Cochliobolus*–*Curvularia* Complex. *Fungal Divers.* **2012**, *56*, 131–144. [[CrossRef](#)]
6. Manamgoda, D.S.; Rossman, A.Y.; Castlebury, L.A.; Crous, P.W.; Madrid, H.; Chukeatirote, E.; Hyde, K.D. The genus *Bipolaris*. *Stud. Micol.* **2014**, *79*, 221–288. [[CrossRef](#)] [[PubMed](#)]
7. Zhang, Y.; Crous, P.W.; Schoch, C.L.; Hyde, K.D. Pleosporales. *Fungal Divers.* **2012**, *53*, 1–221. [[CrossRef](#)] [[PubMed](#)]
8. Berbee, M.L.; Pirseyedi, M.; Hubbard, S. *Cochliobolus* phylogenetics and the origin of known, highly virulent pathogens, inferred from ITS and glyceraldehyde-3-phosphate dehydrogenase gene sequences. *Mycologia* **1999**, *91*, 964–977. [[CrossRef](#)]
9. Castellanos-González, L.; De Mello-Prado, R.; Silva-Campos, C.N.; Barbosada-Silva, J.G. Desarrollo de la mancha foliar por *Bipolaris maydis* (teleomorfo: *Cochliobolus heterostrophus*) en maíz dulce en función de nitrógeno, potasio y silicio en invernadero. *Cienc. Tecnol. Agropecuaria* **2020**, *21*, e1508. [[CrossRef](#)]
10. Romero-Cortes, T.; Zavala-González, E.A.; Pérez, E.V.H.; Aparicio-Burgos, J.E.; Cuervo-Parra, J.A. Characterization of *Cochliobolus sativus* and *Pyrenophora teres* fungi belonging to the leaf spot complex of barley (*Hordeum vulgare*) isolated from barley seeds in Mexico. *Chilean J. Agric. Sci.* **2021**, *37*, 277–289. [[CrossRef](#)]

11. Chen, T.X.; Qi, Y.J.; Wang, L.H.; Li, C.J. First report of leaf spot disease on *Fagopyrum esculentum* caused by *Bipolaris zeae* in China. *Plant Dis.* **2021**, *10*, 3301. [[CrossRef](#)]
12. Pérez-España, V.H.; Cuervo-Parra, J.A.; Aparicio, B.J.E.; Morales-Ovando, M.A.; Peralta, G.M.; Romero-Cortes, T. Importancia de la capa cuticular durante la colonización del hongo causante de la negrilla en *Agave salmiana* Otto ex Salm-Dyck ssp. *salmiana*. *Rev. Mex. Cienc. For.* **2022**, *13*, 158–168. [[CrossRef](#)]
13. Mata-Santoyo, C.I.; Leyva-Mir, S.G.; Camacho-Tapia, M.; Tovar-Pedraza, J.M.; Huerta-Espino, J.; Villaseñor-Mir, H.E.; García-León, E. Aggressiveness of *Bipolaris sorokiniana* and *Alternaria alternata* isolates on wheat cultivars in Mexico. *Rev. Mex. Fitopatol.* **2018**, *36*, 432–443. [[CrossRef](#)]
14. Romero-Cortes, T.; Tamayo-Rivera, L.; Morales-Ovando, M.A.; Aparicio-Burgos, J.E.; Pérez-España, V.H.; Peralta-Gil, M.; Cuervo-Parra, J.A. Growth and yield of purple Kculli corn plants under different fertilization schemes. *J. Fungi* **2022**, *8*, 433. [[CrossRef](#)] [[PubMed](#)]
15. Bockus, W.W.; Bowden, R.L.; Hunger, R.M.; Morrill, W.L.; Murray, T.D.; Smiley, R.W. Diseases caused by fungi and fungus-like organisms. In *Compendium of Wheat Diseases and Pests*, 3rd ed.; The American Phytopathological Society: Saint Paul, MN, USA, 2010; pp. 15–86. [[CrossRef](#)]
16. Manamgoda, D.S.; Cai, L.; Bahkali, A.H.; Chukeatirote, E.; Hyde, K.D. *Cochliobolus*: An overview and current status of species. *Fungal Divers.* **2011**, *51*, 3–42. [[CrossRef](#)]
17. Kobayashi, H.; Sano, A.; Aragane, N.; Fukuoka, M.; Tanaka, M.; Kawaura, F.; Fukuno, Y.; Matsuishi, E.; Hayashi, S. Disseminated infection by *Bipolaris spicifera* in an immunocompetent subject. *Med. Mycol.* **2008**, *46*, 361–365. [[CrossRef](#)] [[PubMed](#)]
18. El Khizzi, N.; Bakshewain, S.; Parvez, S. *Bipolaris*: A plant pathogen causing human infections: An emerging problem in Saudi Arabia. *Res. J. Microbiol.* **2010**, *5*, 212–217. [[CrossRef](#)]
19. Piontelli, L.E. Opportunistic species of clinical relevance in the *Bipolaris* Shoemaker & *Curvularia* Boedijn genera: Its characterization under newest taxonomic criteria. *Taxonomía* **2015**, *30*, 40–63.
20. Carballo, C.M.; Matthews, S.; Spesso, M.F.; Consigli, C. Primer aislamiento en la Argentina de *Bipolaris cynodontis* en la uña. *Dermatol. Argen.* **2018**, *24*, 133–135.
21. Guarner, J.; Brandt, E.M. Histopathologic diagnosis of fungal infections in the 21st century. *Clin. Microbiol. Rev.* **2011**, *24*, 247–280. [[CrossRef](#)]
22. Tan, Y.P.; Crous, P.W.; Shivas, R.G. Eight novel *Bipolaris* species identified from John L. Alcorn's collections at the Queensland Plant Pathology Herbarium (BRIP). *Mycol. Prog.* **2016**, *15*, 1203–1214. [[CrossRef](#)]
23. da Cunha, K.C.; Sutton, D.A.; Fothergill, A.W.; Cano, J.; Gené, J.; Madrid, H.; De Hoog, S.; Crous, P.W.; Guarro, J. Diversity of *Bipolaris* species in clinical samples in the United States and their antifungal susceptibility profiles. *J. Clin. Microbiol.* **2012**, *50*, 4061–4066. [[CrossRef](#)] [[PubMed](#)]
24. Madrid, H.; da Cunha, K.C.; Gené, J.; Dijksterhuis, J.; Cano, J.; Sutton, D.A.; Guarro, J.; Crous, P.W. Novel *Curvularia* species from clinical specimens. *Persoonia* **2014**, *33*, 48–60. [[CrossRef](#)] [[PubMed](#)]
25. Kashyap, A.S.; Manzar, N.; Maurya, A.; Mishra, D.D.; Singh, R.P.; Sharma, P.K. Development of Diagnostic Markers and Applied for Genetic Diversity Study and Population Structure of *Bipolaris sorokiniana* Associated with Leaf Blight Complex of Wheat. *J. Fungi* **2023**, *9*, 153. [[CrossRef](#)] [[PubMed](#)]
26. Manzar, N.; Kashyap, A.S.; Maurya, A.; Rajawat, M.V.S.; Sharma, P.K.; Srivastava, A.K.; Roy, M.; Saxena, A.K.; Singh, H.V. Multi-Gene Phylogenetic Approach for Identification and Diversity Analysis of *Bipolaris maydis* and *Curvularia lunata* Isolates Causing Foliar Blight of Zea mays. *J. Fungi* **2022**, *8*, 802. [[CrossRef](#)] [[PubMed](#)]
27. Mereles, G.L. Calidad Fisiológica, Identificación de Hongos y su Incidencia en la Pudrición de la Mazorca de Maíz *Zea mays* L. en el Municipio de Tepalcing., Morelos. Bachelor's Thesis, Universidad Autónoma Agraria Antonio Narro, Coahuila, México, December 2018.
28. Leyva-Mir, S.G.; Villaseñor-Mir, H.E.; Tovar-Pedraza, J.M.; García-León, E. Respuesta de genotipos de avena a la infección por *Bipolaris victoriae* y *Bipolaris sorokiniana*. *Rev. Mex. Cienc. Agric.* **2019**, *10*, 1023–1034. [[CrossRef](#)]
29. Rodriguez-Pedroso, A.T.; Plascencia-Jatomea, M.; Bautista-Baños, S.; Ventura-Zapata, E.; Cortez-Rocha, M.O.; Ramírez-Arrebato, M.A. Efecto *in vitro* de un quitosano de masa molecular media sobre dos cepas de *Bipolaris oryzae* aisladas en México y Cuba. *Biotecnol. Apl.* **2021**, *38*, 2201–2205.
30. Sivanesan, A. New *Bipolaris*, *Curvularia*, and *Exserohilum* species. *Mycol. Res.* **1992**, *6*, 485–489. [[CrossRef](#)]
31. Hernández, J.J.; Hernández, D.E.M.; López, V.E.; Álvarez, C.J. Aislamiento e identificación del fitopatógeno causal de viruela o “negrilla” en *Agave salmiana* de municipios del estado de Hidalgo, México. *Sci. Fungorum* **2022**, *53*, e1425. [[CrossRef](#)]
32. Ramírez-Cariño, H.F.; Guadarrama-Mendoza, P.C.; Sánchez-López, V.; Cuervo-Parra, J.A.; Ramírez-Reyes, T.I.; Valadez-Blanco, R. Biocontrol of *Alternaria alternata* and *Fusarium oxysporum* by *Trichoderma asperelloides* and *Bacillus licheniformis* in tomato plants. *Anton. Leeuw. Int. J. G.* **2020**, *113*, 1247–1261. [[CrossRef](#)]
33. Marin-Felix, Y.; Groenewald, J.Z.; Cai, L.; Chen, Q.; Marincowitz, S.; Barnes, I.; Bensch, K.; Braun, U.; Camporesi, E.; Damm, U.; et al. Genera of phytopathogenic fungi: GOPHY 1. *Stud. Mycol.* **2017**, *86*, 99–216. [[CrossRef](#)]
34. Cuervo-Parra, J.A.; Sánchez-López, V.; Romero-Cortes, T.; Ramírez-Lepe, M. *Hypocrea/Trichoderma viride* ITV43 with potential for biocontrol of *Moniliophthora roreri* Cif & Par, *Phytophthora megasperma* and *Phytophthora capsici*. *Afr. J. Microbiol. Res.* **2014**, *8*, 1704–1712. [[CrossRef](#)]

35. Romero-Cortes, T.; López-Pérez, P.A.; Pérez, E.V.H.; Medina-Toledo, A.K.; Aparicio-Burgos, J.E.; Cuervo-Parra, J.A. Confrontation of *Trichoderma asperellum* VSL80 against *Aspergillus niger* via the effect of enzymatic production. *Chil. J. Agric. Sci.* **2019**, *35*, 68–80. [[CrossRef](#)]
36. Kendall, J.M.; Rygiewicz, P.T. Fungal-specific PCR primers developed for analysis of the ITS region of environmental DNA extracts. *BMC Microbiol.* **2005**, *5*, 28. [[CrossRef](#)]
37. Zhang, Z.; Schwartz, S.; Wagner, L.; Miller, W. A greedy algorithm for aligning DNA sequences. *J. Comput. Biol.* **2000**, *7*, 203–214. [[CrossRef](#)] [[PubMed](#)]
38. Kumar, S.; Stecher, G.; Li, M.; Knyaz, C.; Tamura, K. MEGA X: Molecular evolutionary genetics analysis across computing platforms. *Mol. Biol. Evol.* **2018**, *35*, 1547–1549. [[CrossRef](#)] [[PubMed](#)]
39. Reveles, H.R.G.; Maldonado, T.C.; Chávez, R.I.; Muñoz, E.J.J.; Moreno, G.A. Vigencia de los Postulados de Koch en la reproducción de *Trichinella spiralis* en modelo experimental. *Rev. Electrón. Vet.* **2014**, *15*, 1–20.
40. Vázquez, D.E.; García, N.J.R.; Peña, V.C.B.; Ramírez, T.H.M.; Morales, R.V. Tamaño de la semilla, emergencia y Desarrollo de la plántula de maguey (*Agave salmiana* Otto ex Salm-Dyck). *Rev. Fitotec. Mex.* **2011**, *34*, 167–173. [[CrossRef](#)]
41. Perelló, A.; Sisterna, M.N.; Cortese, P. Scale for appraising the leaf blight of wheat caused by *Alternaria triticimaculans*. *Cereal Res. Commun.* **1998**, *26*, 189–194. [[CrossRef](#)]
42. Analytical Software, *Statistix 10*, 1st ed.; Analytical Software: Tallahassee, FL, USA, 2017; pp. 7–445.
43. Sisterna, M.; Wolcan, S. *Bipolaris zeae* on *Pennisetum clandestinum* in Argentina. *Summa Phytopathol.* **1990**, *16*, 184–188.
44. Nazareno, d.A.J.R.; d'Avila, C.M.J.; Michalski, M.V.; Rodrigues, R.A.; Santos, S.M.; Saraiva, N.A.S. *Transmissão e Patogenicidade de duas Espécies de Bipolaris Associadas as Sementes de Panicum Maximum Jacq.* 1st ed.; Embrapa Cerrados: Brasilia, Brazil, 2009; p. 16.
45. Xue, L.H.; Liu, Y.; Wu, W.X.; Liang, J.; Zhang, L.; Huang, X.Q.; Zhou, X.Q.; Johnson, R.D.; Li, C.J.; Wang, J.J.; et al. First Report of Leaf Spot of *Hemarthria altissima* Caused by *Bipolaris zeae* in China. *Plant Dis.* **2016**, *101*, 243. [[CrossRef](#)]
46. Minnis, M.A.; Rossman, Y.A.; Kleczewski, M.N.; Flory, L.S. *Bipolaris microstegii* Minnis, Rossman, Kleczewski & S.L. Flory, sp. nov. *Persoonia* **2012**, *29*, 150–151.
47. Sun, X.; Qi, X.; Wang, W.; Liu, X.; Zhao, H.; Wu, C.; Chang, X.; Zhang, M.; Chen, H.; Guoshu, G. Etiology and Symptoms of Maize Leaf Spot Caused by *Bipolaris* spp. in Sichuan, China. *Pathogens* **2020**, *9*, 229. [[CrossRef](#)] [[PubMed](#)]
48. Campos-Rivero, G.; Sánchez-Teyes, L.F.; De la Cruz-Arguijo, E.; Ramírez-González, M.S.; Larralde-Corona, C.P.; Narvaez-Zapata, J.A. Bioprospecting for Fungi with Potential Pathogenic Activity on Leaves of *Agave tequilana* Weber var. Azul. GenBank Direct Submission, 11 October 2018. Available online: <https://www.ncbi.nlm.nih.gov/nucleotide/MK041914.1> (accessed on 1 March 2024).
49. Valencia, Y.T.; Martin, M.R.; Cruz, L.J.R.; Pérez, B.D.; Magaña, A.A.; Cortés, V.A.; Nexticapan, G.A. Identification and Molecular Characterization Phytopathogenic Fungi in *Agave tequilana* in Mexico. GenBank Direct Submission, 2 August 2023. Available online: <https://www.ncbi.nlm.nih.gov/nucleotide/OR388091.1> (accessed on 1 March 2024).
50. Mora-Aguilera, J.A.; Cabrera-Huerta, E.; Nava-Díaz, C.; Hernández-Castro, E. First report of *Epicoccum sorghinum* on Agave Mezcal (*Agave angustifolia*). GenBank Direct Submission, 19 June 2018. Available online: <https://www.ncbi.nlm.nih.gov/nucleotide/MH497563.1> (accessed on 1 March 2024).
51. Cuervo-Parra, J.A.; Romero-Cortes, T.; Aparicio-Burgos, J.E. Isolation and Molecular Identification of Phytopathogenic Fungi, Associated with *Agave salmiana* and *Agave lechuguilla* Plants with Disease Symptoms “Negrilla”, in the State of Hidalgo, Mexico. GenBank Direct Submission, 25 May 2023. Available online: <https://www.ncbi.nlm.nih.gov/nucleotide/OR047544.1> (accessed on 1 March 2024).
52. Campos-Rivero, G.; Sánchez-Teyes, L.F.; De la Cruz-Arguijo, E.; Ramírez-González, M.S.; Larralde-Corona, C.P.; Narvaez-Zapata, J.A. Bioprospecting for Fungi with Potential Pathogenic Activity on Leaves of *Agave tequilana* Weber var. Azul. GenBank Direct Submission, 11 October 2018. Available online: <https://www.ncbi.nlm.nih.gov/nucleotide/MK041894.1> (accessed on 1 March 2024).
53. Cuervo-Parra, J.A.; Romero-Cortes, T.; Aparicio-Burgos, J.E. Isolation and Molecular Identification of Phytopathogenic Fungi, Associated with *Agave salmiana* and *Agave lechuguilla* Plants with Disease Symptoms “Negrilla”, in the State of Hidalgo, Mexico. GenBank Direct Submission, 25 May 2023. Available online: <https://www.ncbi.nlm.nih.gov/nucleotide/OR047545.1> (accessed on 1 March 2024).
54. Flores-Nuñez, N.M.; Camarena-Pozos, D.A.; Partida-Martínez, L.P. Volatiles Emitted by Fungi Associated with the Phyllosphere of Agaves and Cacti are Diverse and Able to Promote Plant Growth. GenBank Direct Submission, 3 April 2020. Available online: <https://www.ncbi.nlm.nih.gov/nucleotide/MT279265.1> (accessed on 1 March 2024).
55. Cuervo-Parra, J.A.; Romero-Cortes, T.; Aparicio-Burgos, J.E. Isolation and Molecular Identification of Phytopathogenic Fungi, Associated with *Agave salmiana* and *Agave lechuguilla* Plants with Disease Symptoms “Negrilla”, in the State of Hidalgo, Mexico. GenBank Direct Submission, 25 May 2023. Available online: <https://www.ncbi.nlm.nih.gov/nucleotide/OR047542.1> (accessed on 1 March 2024).
56. Tapia-Tussell, R.; Solis, S.; Pérez-Brito, D. Identification and Molecular Characterization of Ligninolytic Fungi from Yucatan, Mexico. GenBank Direct Submission, 17 June 2009. Available online: <https://www.ncbi.nlm.nih.gov/nucleotide/GQ280375.1> (accessed on 1 March 2024).
57. Cuervo-Parra, J.A.; Romero-Cortes, T.; Aparicio-Burgos, J.E. Isolation and Molecular Identification of Phytopathogenic Fungi, Associated with *Agave salmiana* and *Agave lechuguilla* Plants with Disease Symptoms “Negrilla”, in the State of Hidalgo, Mex-

- ico. GenBank Direct Submission, 25 May 2023. Available online: <https://www.ncbi.nlm.nih.gov/nucleotide/OR047532.1> (accessed on 1 March 2024).
58. Mohammadi, A.; Amini, Y. Molecular characterization and identification of *Acrostalagmus luteoalbus* from Saffron in Iran. *Agric. Sci. Dev.* **2015**, *4*, 16–18.
59. Toju, H.; Tanabe, A.S.; Yamamoto, S.; Sato, H. High-coverage ITS primers for the DNA-based identification of ascomycetes and basidiomycetes in environmental samples. *PLoS ONE* **2012**, *7*, e40863. [CrossRef] [PubMed]
60. Morgulis, A.; Coulouris, G.; Raytselis, Y.; Madden, T.L.; Agarwala, R.; Schäffer, A.A. Database indexing for production MegaBLAST searches. *Bioinformatics* **2008**, *24*, 1757–1764. [CrossRef] [PubMed]
61. Visagie, C.M.; Bhiya, T.; Kgatle, G. *Alternaria* Diversity from South Africa. GenBank Direct Submission. 22 May 2020. Available online: <https://www.ncbi.nlm.nih.gov/nucleotide/MT505870.1> (accessed on 10 June 2022).
62. Vu, D.; Groenewald, M.; de Vries, M.; Gehrmann, T.; Stielow, B.; Eberhardt, U.; Al-Hatmi, A.; Groenewald, J.Z.; Cardinali, G.; Houbraken, J.; et al. Large-scale generation and analysis of filamentous fungal DNA barcodes boosts coverage for kingdom fungi and reveals thresholds for fungal species and higher taxon delimitation. *Stud. Mycol.* **2019**, *92*, 135–154. [CrossRef] [PubMed]
63. Berbee, M.L. Molecular Phylogenetics of *Cochliobolus*. GenBank Direct Submission, 30 July 1998. Available online: <https://www.ncbi.nlm.nih.gov/nuccore/af081452> (accessed on 13 June 2022).
64. Bohl, S.K.; Harmon, P.F.; Clay, K.; Goss, E.M.; Flory, S.L. Widespread Independent Emergence and Accumulation of Fungal pathogens Reduce Fecundity of an Invasive Grass. GenBank Direct Submission, Submitted 10 August 2014. Available online: <https://www.ncbi.nlm.nih.gov/nuccore/km507725> (accessed on 13 June 2022).
65. Adetunji, M.C.; Mwanza, M. Fungal Profile of Groundnut sold in Mafikeng, North West, South Africa. GenBank Direct Submission, 26 April 2019. Available online: <https://www.ncbi.nlm.nih.gov/nuccore/mk841439> (accessed on 13 June 2022).
66. Berbee, M.; Pirseyedi, M.; Hubbard, S. GenBank Direct Submission. 10 June 1998. Available online: <https://www.ncbi.nlm.nih.gov/nuccore/af071325> (accessed on 13 June 2022).
67. Berbee, M.; Pirseyedi, M.; Hubbard, S. GenBank Direct Submission. 10 June 1998. Available online: <https://www.ncbi.nlm.nih.gov/nuccore/af071329> (accessed on 13 June 2022).
68. Ahmadpour, A.; Donyadoost-Chelan, M.; Heidarian, Z.; Javan-Nikkah, M. New species of *Bipolaris* and *Curvularia* on grass species in Iran. *Rostaniha* **2011**, *12*, 39–49.
69. Staiger, S.; Seufert, P.; Arand, K.; Burghardt, M.; Popp, C.; Riederer, M. The permeation barrier of plant cuticles: Uptake of active ingredients is limited by very long-chain aliphatic rather than cyclic wax compounds. *Pest Manag. Sci.* **2019**, *75*, 3405–3412. [CrossRef]
70. Pérez-España, V.H.; Cuervo-Parra, J.A.; Paz-Camacho, C.; Morales-Ovando, M.A.; Gómez-Aldapa, C.A.; Rodríguez-Jiménez, G.C.; Robles-Olvera, V.J.; López-Pérez, P.A.; Romero-Cortes, T. General characterization of cuticular membrane isolated from *Agave salmiana*. *Int. J. Bio-resour. Stress Manag.* **2019**, *10*, 046–052. [CrossRef]
71. Centro Internacional de Mejoramiento de Maíz y Trigo (CIMMYT). *Enfermedades del Maíz: Una Guía Para su Identificación en el Campo*, 4th ed.; CIMMYT: Ciudad de México, Mexico, 2004; pp. 18–33.
72. Cuervo-Parra, J.A.; Romero-Cortes, T.; Aparicio-Burgos, J.E. Isolation and Molecular Identification of phytopathogenic Fungi, Associated with *Agave salmiana* and *Agave lechuguilla* Plants with Disease Symptoms “Negrilla”, in the State of Hidalgo, Mexico. GenBank Direct Submission, 25 May 2023. Available online: <https://www.ncbi.nlm.nih.gov/nucleotide/OR047538.1> (accessed on 1 March 2024).
73. Cuervo-Parra, J.A.; Romero-Cortes, T.; Aparicio-Burgos, J.E. Isolation and Molecular Identification of Phytopathogenic Fungi, Associated with *Agave salmiana* and *Agave lechuguilla* Plants with Disease Symptoms “Negrilla”, in the State of Hidalgo, Mexico. GenBank Direct Submission, 25 May 2023. Available online: <https://www.ncbi.nlm.nih.gov/nucleotide/OR047536.1> (accessed on 1 March 2024).

**Disclaimer/Publisher’s Note:** The statements, opinions and data contained in all publications are solely those of the individual author(s) and contributor(s) and not of MDPI and/or the editor(s). MDPI and/or the editor(s) disclaim responsibility for any injury to people or property resulting from any ideas, methods, instructions or products referred to in the content.